Practical Evaluation of Polymer Waveguides for High-Speed and Meter-Scale On-Board Optical Interconnects

Xiao Xu[®], Lin Ma[®], *Member, IEEE*, Marika Immonen, *Member, IEEE*, Xinhong Shi, *Member, IEEE*, Brandon W. Swatowski[®], Jon V. DeGroot, and Zuyuan He[®], *Senior Member, IEEE, Member, OSA*

Abstract-We comprehensively evaluated optical characteristics, environmental stabilities, fiber optics compatibilities, and high-speed performances of multimode polymer waveguides fabricated in small batch with a length of 946 mm. The waveguides exhibit a low transmission loss (0.046 dB/cm at a wavelength of 850 nm), low interchannel crosstalk (≤ -58 dB), and a large misalignment tolerance ($\pm 20~\mu m$) between fiber and waveguide. The waveguides show good environmental stability and the increase of propagation loss is as small as 0.005 dB/cm and 0.004 dB/cm after a 1000-h ageing test and five solder reflow cycles, respectively. The waveguides have good compatibilities with fibers having different core diameters and index profiles that may be encountered in the real application environment. High-speed transmission performances were evaluated using both nonreturn to zero (NRZ) transmission at data rates of 25 Gb/s and 30 Gb/s, and PAM4 transmission at data rates of 20 Gb/s and 56 Gb/s, respectively. There is no obvious degradation on the eye diagram due to the insertion of the waveguide. Error free transmission were successfully obtained for NRZ transmission at data rates of both 25 Gb/s and 30 Gb/s. The BER for PAM4 transmission reached a level of 10⁻⁴ at data rates of both 10 Gbaud (20 Gb/s) and 28 Gbaud (56 Gb/s), which is well below the forward error correction limitation. Moreover, it is the bandwidth of the test equipment rather than the polymer waveguide itself that limits the high-speed transmission performances in our experiments. The results demonstrate that the polymer waveguides are good candidates for high-speed and meter-scale on-board optical interconnect applications.

Index Terms—Electric-optical printed circuit boards, optical interconnects, optical polymers, optical waveguides.

Manuscript received July 11, 2017; revised December 12, 2017 and April 24, 2018; accepted May 29, 2018. Date of publication June 19, 2018; date of current version June 29, 2018. This work was supported by the National Natural Science Foundation of China (NSFC) under Grants 61775138 and 61620106015. (Corresponding author: Lin Ma.)

X. Xu, L. Ma, and Z. He are with the State Key Laboratory of Advanced Optical Communication Systems and Networks, Shanghai Jiao Tong University, Shanghai 200240, China (e-mail: xiao2014@sjtu.edu.cn; ma.lin@sjtu.edu.cn; zuyuanhe@sjtu.edu.cn).

M. Immonen is with TTM Technologies, Salo 24100, Finland (e-mail: marika.immonen@ttmtech.com.hk).

X. Shi is with the TTM Technologies, Shanghai 201613, China (e-mail: xinhong.Shi@smst.ttmtech.com.cn).

B. W. Swatowski and J. V. DeGroot are with the Dow Corning Corporation, Midland, MI 48686 USA (e-mail: brandon.swatowski@dowcorning.com; jon.degroot@dowcorning.com).

Color versions of one or more of the figures in this paper are available online at http://ieeexplore.ieee.org.

Digital Object Identifier 10.1109/JLT.2018.2847461

I. INTRODUCTION

HE increasing operation speed of datacenters and high performance computers gives ever-increased burden on the bandwidth of intra-system interconnects [1]–[3]. High function application specific integrated circuits (ASICs), such as switch chips, are driving requirements for higher I/O density and lower interface power. In typical high speed serial link, channel length can reach 1 meter in backplane channels and 5 meters in copper cable channels. Current designs deploy 25 Gb/s SerDes in high speed links, but next generation electrical and optical 50 Gb/s and 56 Gb/s single lane interconnect standards are under definition by IEEE 802.3bs and OIF CEI-56G-VSR [4], [5]. Signal integrity is impacted by many impairments such as jitter, noise, frequency-dependent loss, reflections, and crosstalk at higher frequencies. A viable solution to scale up data rate is to use higher order modulation. 4-level pulse amplitude modulation (PAM4) can double the channel bandwidth with the same signaling rate compared with binary non-return to zero (NRZ), and is exploited as the path for narrower 200 G (4 \times 50 G) and 400 G (8 × 50 G) module interfaces compared with NRZ $(16 \times 25 \text{ G})$ configurations. Moreover, CEI-112G-VSR to develop 100 G single lane implementation agreement for chip-tomodule interface has already been launched.

Optical interconnects have drawn significant attentions owing to their advantages over conventional electronic solutions in various aspects, such as broad bandwidth, high density, low power consumption, low cost and immunity to electromagnetic interference [6], [7]. Various optical technologies have been proposed, including free-space optical interconnects [8], [9], optical fiber wiring technology [10], [11], planar waveguide technology [12]–[15] and silicon photonics [16], [17].

In order to meet the future requirements, intensive research and standardization activities such as Phoxtrot, HDPUG, IEC TC86 JWG9 on short reach optical technologies have been carrying out to replace intra-system electrical links by optical means [18]–[21]. Fig. 1 shows objected architecture using optical interconnects for intra-rack high-speed links. Multimode optical waveguides combined with on-board optical engines located close to host chip on card are considered to be near term solution for chip-to-chip interconnects over optical backplane. Single-mode waveguides and silicon photonics are considered to be longer term solutions [22].

0733-8724 © 2018 IEEE. Personal use is permitted, but republication/redistribution requires IEEE permission. See http://www.ieee.org/publications_standards/publications/rights/index.html for more information.

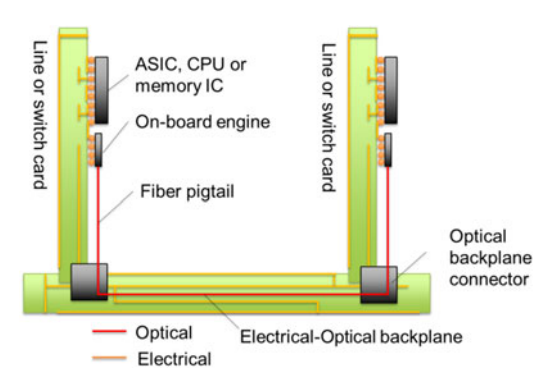


Fig. 1. System architecture with optical intra-system links.

Near-term implementation makes use of 850 nm optical engines which are widely available from multiple vendors on the market with several lane options ($\times 4$, $\times 8$, $\times 12$, $\times 16$) and data rates (up to 28 Gb/s per lane). Vertical cavity surface emitting lasers (VCSELs) have been demonstrated with data rates over 50 Gb/s [23], [24]. However, the stringent loss budget with higher data rate pose particular challenges for link loss and signal integrity characteristics.

As a result, multimode polymer waveguides play an important role in high-speed on-board optical interconnect applications. They have good compatibilities with both printed circuit boards (PCBs) and fiber optics. They can be embedded inside or laminated on the surface of PCBs and can be coupled with graded-index (GI) multimode fibers with a low coupling loss [25]. The large core dimensions relax the alignment tolerances, and therefore, reduce cost for packaging and connection. However, signal degradation due to their highly multimode nature leaves concerns on both transmission data rate and applicable distance [26]. The bandwidth-length product and highspeed data transmission of meter-scale multimode waveguides have been investigated [27], [28]. Bandwidth-length product of >40 GHz·m without the need for any specific launch conditioning has been obtained [29], and 56 Gb/s PAM-4 data transmission has been demonstrated [30]. On the other hand, the environmental stability of the polymer waveguides is another concern for practical applications.

In this paper, we studied the performance of multimode polymer waveguides for high-density and meter-scale on-board optical interconnects. We measured the transmission loss, interchannel crosstalk, misalignment tolerance of the waveguides and studied their environmental stability and compatibilities with fiber optics. Moreover, we evaluated the high-speed transmission performances using both NRZ data transmission at rates of 25 Gb/s and 30 Gb/s, and PAM4 data transmission at rates of 20 Gb/s and 56 Gb/s, respectively.

II. OPTICAL CHARACTERISTICS

We used sets of polymer waveguides in spiral design fabricated on silicon substrate using photo curable silsequioxane materials (Dow Corning WG-1022 Optical Waveguide Core, Dow Corning WG-1025 Optical Waveguide Clad, Dow Corning WG-1027 Optical Waveguide Clad) for evaluation. The

TABLE I REFRACTIVE INDICES

Material	850 nm	1310 nm
WG-1022	1.526	1.519
WG-1025	1.507	1.503
WG-1027	1.502	1.497

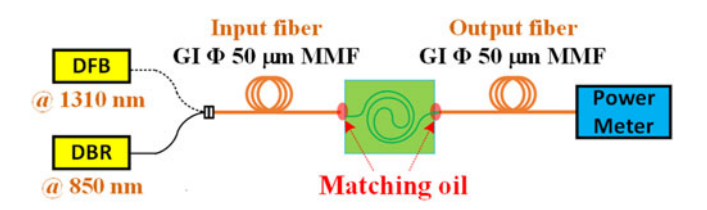


Fig. 2. Experimental setup for propagation loss measurement.

refractive indices are listed in Table I. On a single piece of the waveguide chip, there are 6 long and 6 short (for reference purposes) spiral channels with a length of 946 mm and 162.5 mm, respectively. The core size is approximately $52 \times 54 \ \mu \text{m}^2$. The pitch of the waveguides is $250 \ \mu \text{m}$ which coincides with that of the VCSELs, photodiode arrays and multimode fiber ribbons.

A. Propagation Loss

The experimental setup for insertion loss measurement is shown in Fig. 2. Two distributed Bragg reflector laser diodes (DBR-LDs) working at 850 and 1310 nm, respectively, were used as the light source. Light from the laser diodes was buttcoupled into and out from the waveguides using 2-meter long 50- μ m-core GI fibers. Matching oil with a refractive index of 1.47 at a wavelength of 1550 nm was applied on both the input and the output facets to reduce the coupling loss. Since both the waveguide width and the facet processing condition for the long and short waveguides are exactly the same, we assume that the coupling loss between the waveguides and the optical fibers are identical. As a result, both the propagation loss of the waveguides and the coupling loss between the waveguides and optical fibers can be worked out through measuring the insertion loss of both the short and long waveguides. In our experiment, all 12 waveguides on the substrate were measured and the results are shown in Fig. 3. The error bar in the figure represent the power deviation of the channels. The average propagation losses derived from the slope of the measured insertion losses at 850 nm and 1310 nm are 0.046 dB/cm and 0.342 dB/cm, respectively, and the total coupling loss of both the input and the output port is about 0.5 dB.

B. Inter-Channel Crosstalk

Inter-channel crosstalk, which will cause severe degradation on transmitted signal, are resulted from mode coupling and mode conversion between adjacent waveguides. Since the waveguides under test have a pitch as large as 250 μ m, the inter-channel crosstalk is mainly caused by the mode conversion, which attributes to the coupling of the cladding scattered

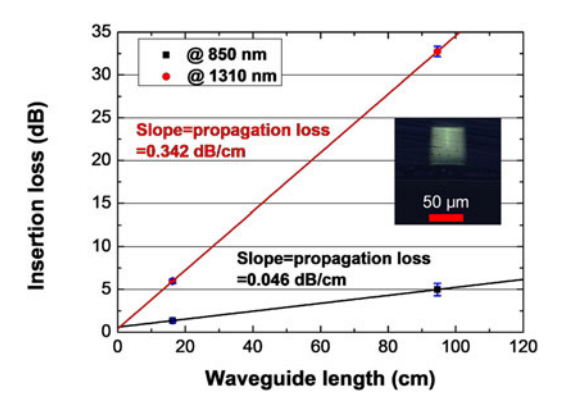


Fig. 3. Insertion loss measurement for two waveguides with a length of 946 mm and 162.5 mm, respectively, at both 850 nm and 1310 nm. The inset shows the micrograph of the end facet.

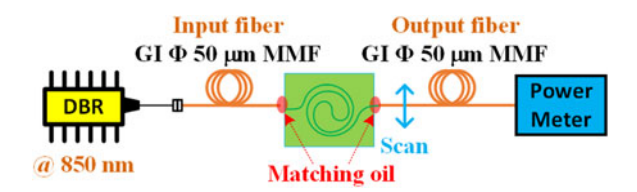


Fig. 4. Experimental setup for crosstalk measurement.

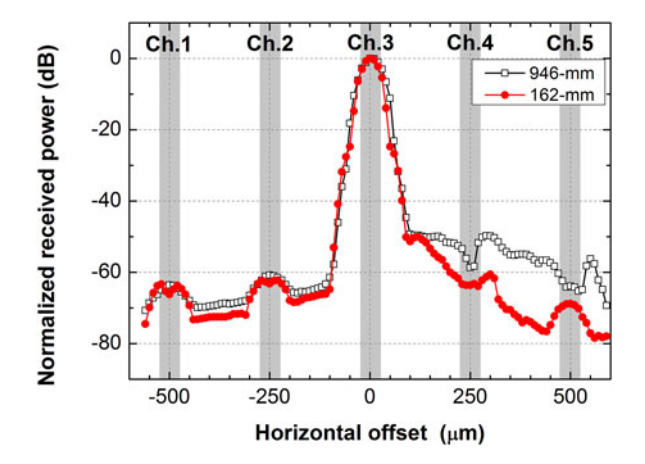


Fig. 5. Normalized received optical power at the output side as a function of the horizontal offset of output fiber. The gray stripes represent the position of the waveguides.

light due to surface roughness, bending and other imperfections of the waveguides.

The inter-channel crosstalk at 850 nm was measured using experimental setup depicted in Fig. 4. The experimental setup and conditions are the same as that for insertion loss measurement except that the output fiber was scanned in the horizontal direction with a step of $10~\mu m$ in order to record the optical power at different positions.

The experimental results are shown in Fig. 5. The light was center launched into Channel 3 (Ch.3) from a 50- μ m-core GI fiber with matching oil applied on both the input and the output ports. It can be observed that the maximum interchannel crosstalk measured at the output port of the 946-mm and 162.5-mm-long waveguides are as low as -58 dB (Ch.4) and -62 dB (Ch.2), respectively, which indicates that inter-channel

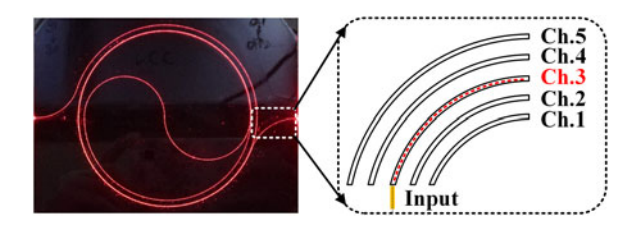


Fig. 6. Photograph of spiral waveguides and the schematic of the waveguide bending at the output port.

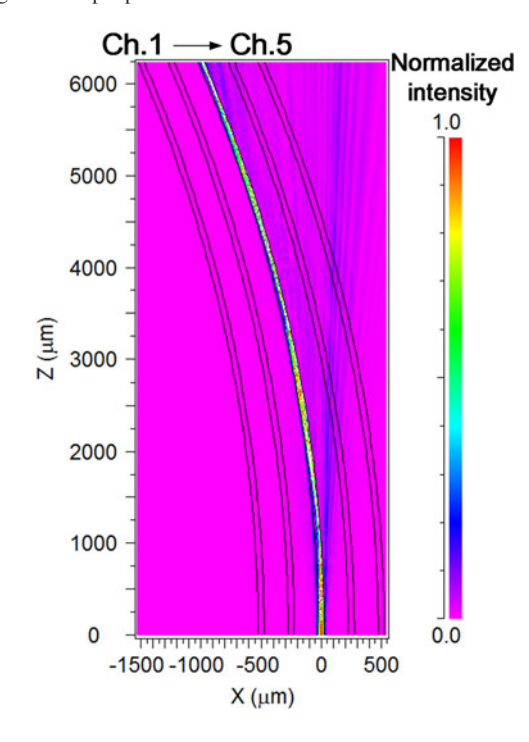


Fig. 7. Crosstalk simulation result of bending waveguides.

crosstalk characteristic of the fabricated waveguides well satisfied the requirement for on-board optical interconnect applications. Compared to the earlier result of approximately -35 dB for 125-mm-long straight waveguides [31], the inter-channel crosstalk observed in our experiments are smaller. The difference in crosstalk may be attributed to the changes in measurement parameters such as launch conditions and the length and shape (straight vs. spiral) of the waveguides, as well as the improvement in both the optical properties of the raw materials and fabrication process of the waveguides.

The detected light power coupled to the adjacent channels decreases with the increase of the distance apart from the input channel. Moreover, the light power in the cladding structure of the outer side waveguides (Ch.4 and Ch.5) is 10 to 15 dB higher than that of the inner side waveguides (Ch.1 and Ch.2). This is due to the bending direction of the spiral waveguides as shown in Fig. 6. The simulated result conducted under the same condition with the fabricated waveguides using a beam propagation method is also shown in Fig. 7. The light leaked from the outer side of the bending structure and resulted in a higher detected power in the outer side cladding. However, instead of directly coupling into the adjacent channels, most of the leaked light in the cladding penetrated the adjacent channels

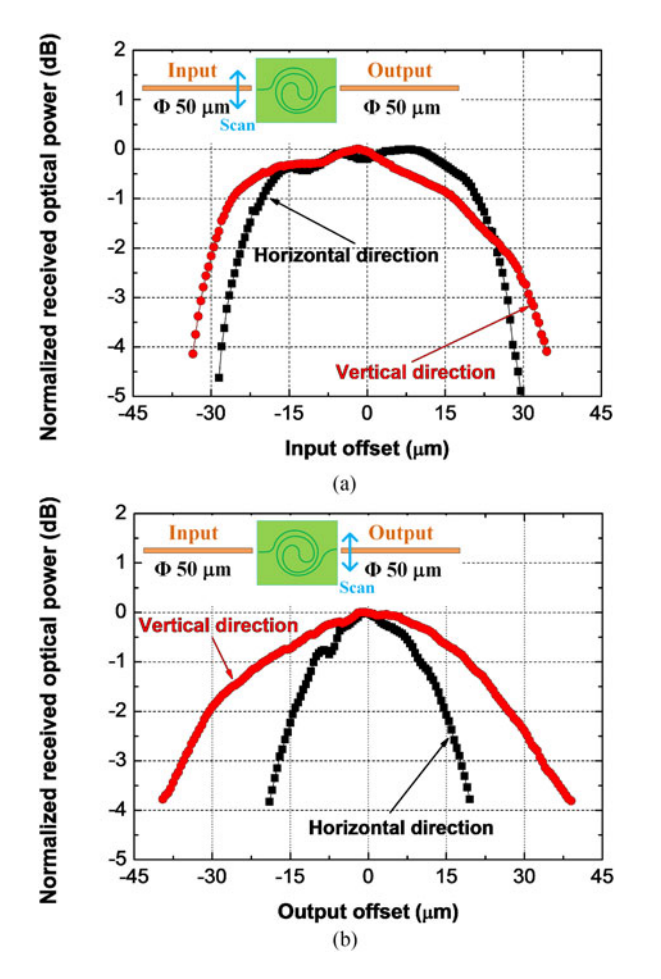


Fig. 8. Normalized received power as functions of misalignment in both horizontal and vertical directions for (a) input, and (b) output fiber.

and did not cause a significant increase of the inter-channel crosstalk in the adjacent channels in the outer side.

C. Misalignment Tolerance

Misalignment tolerance at the input side was measured by keeping the output fiber fixed and scanning the input fiber with a step of 0.5 μ m in both horizontal and vertical directions using the same experimental setup for crosstalk measurements as shown in Fig. 4. The received power as a function of the displacement of the input fiber is shown in Fig. 8(a). The 3 dB misalignment tolerances for horizontal and vertical direction are ± 27 and $\pm 31~\mu$ m, respectively. When keeping the input fiber at the center launching position and scanning the output fiber, the observed 3 dB misalignment tolerances for horizontal and vertical direction as shown in Fig. 8(b) are ± 20 and $\pm 32~\mu$ m, respectively.

It can be observed that the input fiber misalignment tolerance in the horizontal direction is approximately 7 μm larger than that for the output one. This can be explained by the result of near field pattern (NFP) observation of the waveguide as shown in Fig. 13(b). In the horizontal direction, instead of a uniform distribution, large portion of the power is distributed in the center of the core which results in a tighter misalignment tolerance.

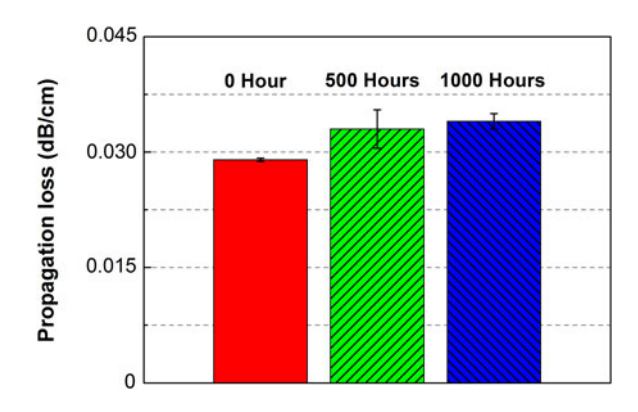


Fig. 9. Propagation loss of waveguides before and after ageing test.

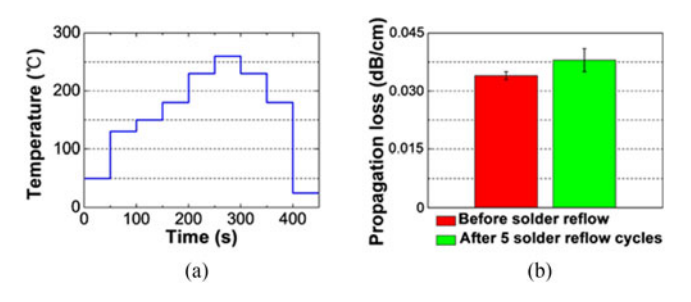


Fig. 10. (a) Solder reflow profile used in thermal analysis; (b) Propagation losses before and after 5 solder reflow cycles.

III. ENVIRONMENTAL STABILITIES

In order to investigate the environmental stability of the waveguides, ageing test was carried out using sets of the waveguides under a condition of a relative humidity of 85% and a temperature of 85 °C which is commonly referred as 85% RH/85 °C ageing test. Fig. 9 shows that after the ageing test of 500 and 1000 hours, the propagation loss increase is as small as 0.004 and 0.005 dB/cm respectively at a wavelength of 850 nm.

Five runs of solder reflow were also performed on sets of the waveguides to assess the impact that reflow will have on embedded waveguides in the PCB manufacturing environment. The reflow condition that the sample was subjected to was a 50 °C/130 °C/150 °C/180 °C/230 °C/260 °C/230 °C/180 °C profile with the sample at each temperature for 50 seconds as shown in Fig. 10(a). Pre- and post-solder reflow insertion loss testing showed that a net increase of 0.004 dB/cm in propagation loss at 850 nm was observed as shown in Fig. 10(b) after five reflow cycles were performed.

IV. FIBER OPTICS COMPATIBILITIES

The fiber optics compatibilities were evaluated by carrying out a bit error rate (BER) test on the 946-mm-long waveguide using 4 typical optical fibers, namely, 9- μ m-core standard single-mode fiber (SSMF), 50- μ m-core graded-index fibers (OM2 and OM3 fibers), and 62.5- μ m-core graded-index fibers (OM1 fiber) that may be encountered in the practical systems as launching fibers. The experimental setup for BER test is shown in Fig. 11. Fibers for launching compatibility test was directly butt-coupled to the waveguides and an OM2 fiber was fixed at the output side as the receiving fiber with matching oil applied to both of the

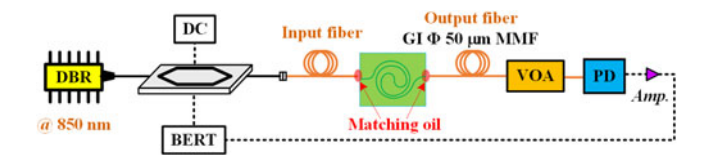


Fig. 11. Experimental setup for launching fiber compatibility test.

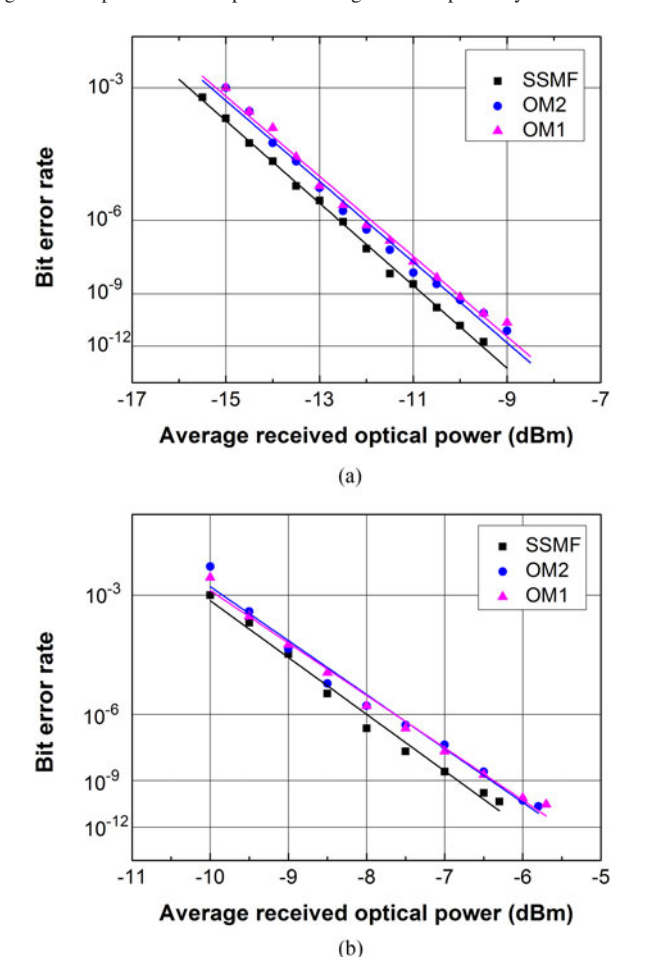


Fig. 12. BER test of the 946-mm-long waveguide using SSMF, OM1, and OM2 fibers as launching fibers at a data rate of (a) 10 Gb/s and (b) 25 Gb/s, respectively.

input and the output ports. The bit error ratio tester (BERT, multilane ML 4009) generates electrical NRZ signal with a pseudo-random binary sequence (PRBS) length of 2^7-1 at data rates of 10 Gb/s or 25 Gb/s. Light from the DBR-LD at 850 nm was coupled to the intensity modulator with a bandwidth of 25 GHz together with the NRZ signal and a direct current (DC) driving signal. A multimode variable optical attenuator (VOA) was used for optical power adjustment. The light from the VOA was detected using a photodiode with a bandwidth of 22 GHz. After amplifying by a 50 GHz RF amplifier, the electrical signal from the PD was fed back to the BERT for analysis.

The result of BER test at a data rate of 10 Gb/s and 25 Gb/s using SSMF, OM1, and OM2 fibers as launching fibers are shown in Fig. 12(a) and (b), respectively. Compared with SSMF, when using OM1, OM2 fibers as launching fibers, the transmission performance slightly degrade, and the power penalties

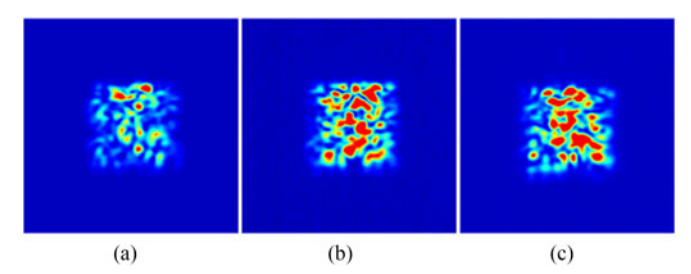


Fig. 13. Output near field patterns of the waveguide with (a) SSMF, (b) OM2 fiber, and (c) OM1 fiber as the launching fiber.

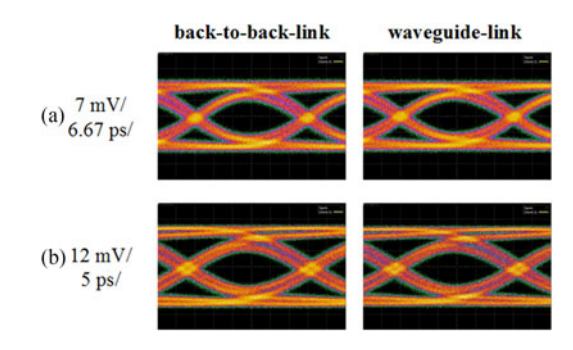


Fig. 14. Eye diagrams at (a) 25 Gb/s and (b) 30 Gb/s. The voltage and time scale of the recorded eye diagrams are noted.

observed at 10^{-9} were 0.6 dB and 0.4 dB for 10 Gb/s and 25 Gb/s, respectively. The difference in using OM1 or OM2 fibers as launching fiber is small, and since the difference between using OM2 and OM3 fibers as launching fiber is negligible, we omitted the results of OM3 fibers for obtaining better visibility of the figures.

The observed output NFPs of the waveguide at a wavelength of 1310 nm using SSMF, OM1, and OM2 as the launching fibers are shown in Fig. 13. The input power for all the experiments are kept the same. Due to the smaller core size and single-mode characteristic of the SSMF, the majority of the light power was located in the center of the waveguide and smaller number of modes were stimulated when using SSMF as the launching fiber compared with that using OM1 and OM2 fibers. This result agrees with that of BER observation that using SSMF as the launching fiber can achieve a better BER performance.

V. HIGH-SPEED PERFORMANCES

To evaluate the high-speed performance of the waveguide at 850 nm, both NRZ transmission (at data rates of 25 Gb/s and 30 Gb/s) and PAM4 transmission (at data rates of 20 Gb/s and 56 Gb/s) were implemented on a 946-mm-long waveguide.

A. NRZ

The experimental setup shown in Fig. 11 was used for NRZ transmission, and $50-\mu m$ -core fibers were used as the coupling fibers for both the input and output port. The performance of back-to-back link was also measured. The eye diagrams were measured using the sampling oscilloscope (KEYSIGHT DCA-X 86100D) and the results are shown in Fig. 14. The voltage and time scale of the diagrams were also recorded and

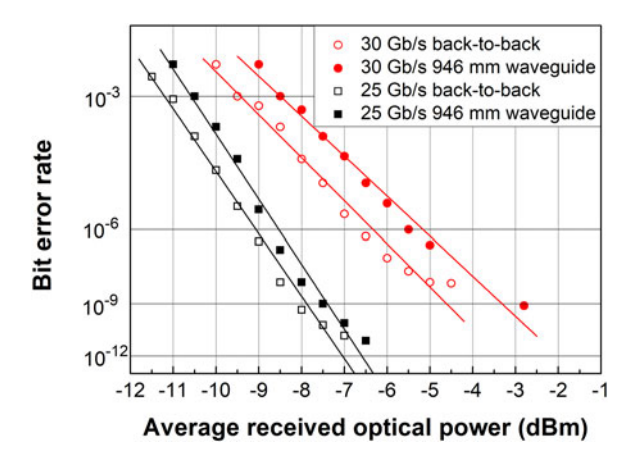


Fig. 15. BER curves of NRZ data transmission at 25 Gb/s and 30 Gb/s.

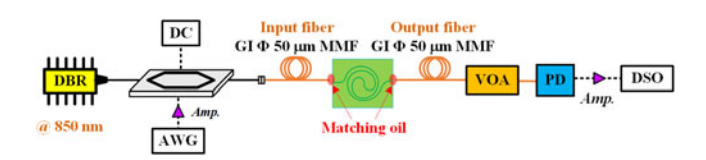


Fig. 16. Experimental setup for PAM4 transmission.

the average received optical power is -6 dBm and -3 dBm at a data rate of 25 Gb/s and 30 Gb/s, respectively. There is no obvious degradation of the eye diagrams due to the insertion of the waveguide. The obtained BER curves at both data rates are shown in Fig. 15. Error free transmission were successfully obtained at data rates of both 25 Gb/s and 30 Gb/s. It can be observed that the power penalty for BER of 10^{-9} due to the insertion of the waveguide is as small as 0.5 dB and 1.3 dB at a data rate of 25 Gb/s and 30 Gb/s, respectively.

B. PAM4

The PAM4 transmission were implemented using experimental setup as shown in Fig. 16. The arbitrary waveform generator (AWG, KEYSIGHT M8195A) was used to generate PAM4 signal. The coupling condition of the waveguide was exactly the same as that for NRZ transmission test. The electrical signal after amplification was captured by a digital storage oscilloscope (DSO, KEYSIGHT DSOZ592A) and the BERs were counted offline. PAM4 transmission tests at 10 Gbaud (20 Gb/s) and 28 Gbaud (56 Gb/s) were done and the results are shown in Fig. 17. The average received optical power is -5.5 dBm and −2 dBm for 10 Gbaud and 28 Gbaud, respectively. There is no obvious degradation of the eye diagram due to the insertion of the waveguide. However, a relative eye closure at 56 Gb/s for both back-to-back and waveguide link were observed due to the low received power. The result for the BER measurement is shown in Fig. 18. The BER reached a level of 10^{-4} for both 10 Gbaud (20 Gb/s) and 28 Gbaud (56 Gb/s) transmission, which is well below the forward error correction (FEC) limitation. Moreover, the polymer waveguide itself is not the main factor that limits the high-speed transmission performances.

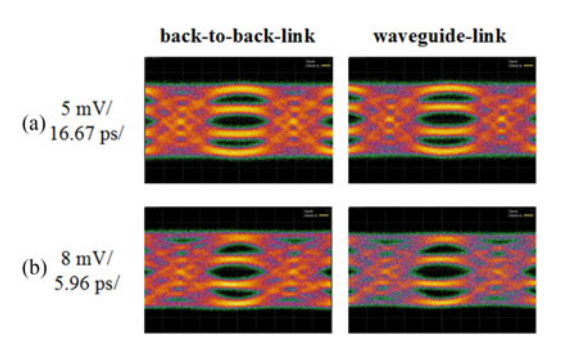


Fig. 17. Eye diagrams at (a) 10 Gbaud (20 Gb/s) for average received optical power of -5.5 dBm and (b) 28 Gbaud (56 Gb/s) for average received optical power of -2 dBm. The voltage and time scale of the recorded eye diagrams are noted

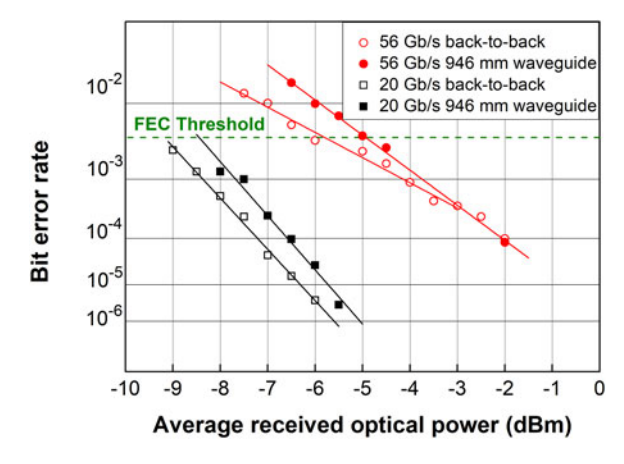


Fig. 18. BER curves of PAM4 data transmission at 10 Gbaud (20 Gb/s) and 28 Gbaud (56 Gb/s).

VI. CONCLUSION

We comprehensively studied the practicability of polymer waveguides for high-speed meter-scale on-board optical interconnect applications. Low transmission loss (0.046 dB/cm at a wavelength of 850 nm), low inter-channel crosstalk (\leq -58 dB) and large misalignment tolerance ($\pm 20 \mu m$) are achieved. The waveguides show good environmental stability and the increase of propagation loss is as small as 0.005 and 0.004 dB/cm after a 1000-hour ageing test and five solder reflow cycles, respectively. Good compatibilities with the fibers have been observed by using launching fibers with different core diameters and index profiles that may be encountered in the real application environment. To evaluated high-speed transmission performances of the waveguides, we measured the BRE curves and eye diagrams of both NRZ data at rates of 25 and 30 Gb/s, and PAM4 data at rates of 20 and 56 Gb/s, respectively. There is no obvious degradation on the eye diagram due to the insertion of the waveguide. Error free transmission and open eye diagrams were successfully obtained for NRZ transmission at data rates of both 25 and 30 Gb/s. The BER for PAM4 transmission reached a level of 10^{-4} at data rates of both 10 Gbaud (20 Gb/s) and 28 Gbaud (56 Gb/s), which is well below the forward error correction limitation. The results imply that the polymer waveguides are promising for high-speed on-board optical interconnect applications.

REFERENCES

- C. Li, M. Browning, P. V. Gratz, and S. Palermo, "LumiNOC: A power-efficient, high-performance, photonic network-on-chip," *IEEE Trans. Comput.-Aided Design Integr. Circuits Syst.*, vol. 33, no. 6, pp. 826–838, Jun. 2014.
- [2] S. B. Yoo, "The role of photonics in future computing and data centers," IEICE Trans. Commun., vol. 97, no. 7, pp. 1272–1280, Jul. 2014.
- [3] A. F. Benner, P. K. Pepeljugoski, and R. J. Recio, "A roadmap to 100G Ethernet at the enterprise data center," *IEEE Commun. Mag.*, vol. 45, no. 11, pp. 10–17, Nov. 2007.
- [4] IEEE P802.3bs 400 Gb/s Ethernet Task Force, 2014. [Online]. Available: http://www.ieee802.org/3/bs/
- [5] J. He et al., Programmable virtual transport network services specification, 2015. [Online]. Available: http://www.oiforum.com/ technicalwork/current-oif-work/
- [6] D. A. Miller, "Rationale and challenges for optical interconnects to electronic chips," *Proc. IEEE*, vol. 88, no. 6, pp. 728–749, Jun. 2000.
- [7] E. D. Kyriakis-Bitzaros, N. Haralabidis, M. Lagadas, A. Georgakilas, Y. Moisiadis, and G. Halkias, "Realistic end-to-end simulation of the optoelectronic links and comparison with the electrical interconnections for system-on-chip applications," *J. Lightw. Technol.*, vol. 19, no. 10, pp. 1532–1542, Oct. 2001.
- [8] K. Wang, A. Nirmalathas, C. Lim, E. Skafidas, and K. Alameh, "High-speed free-space based reconfigurable card-to-card optical interconnects with broadcast capability," *Opt. Express*, vol. 21, no. 13, pp. 15395–15400, Jun. 2013.
- [9] M. Jarczynski, T. Seiler, and J. Jahns, "Integrated three-dimensional optical multilayer using free-space optics," *Appl. Opt.*, vol. 45, no. 25, pp. 6335–6341, Sep. 2006.
- [10] I. K. Cho, J. H. Ryu, and M. Y. Jeong, "Interchip link system using an optical wiring method," *Opt. Lett.*, vol. 33, no. 16, pp. 1881–1883, Aug. 2008.
- [11] J. Matsui et al., "High bandwidth optical interconnection for densely integrated server," in Proc. Opt. Fiber Commun. Conf., Anaheim, CA, USA, 2013, pp. 1–3.
- [12] A. Hashim, N. Bamiedakis, R. V. Penty, and I. H. White, "Multimode polymer waveguide components for complex on-board optical topologies," *J. Lightw. Technol.*, vol. 31, no. 24, pp. 3962–3969, Dec. 2013.
- [13] R. Dangel et al., "Development of versatile polymer waveguide flex technology for use in optical interconnects," J. Lightw. Technol., vol. 31, no. 24, pp. 3915–3926, Dec. 2013.
- [14] K. Schmidtke et al., "960 Gb/s optical backplane ecosystem using embedded polymer waveguides and demonstration in a 12G SAS storage array," J. Lightw. Technol., vol. 31, no. 24, pp. 3970–3975, Dec. 2013.
- [15] R. C. A. Pitwon et al., "Pluggable electro-optical circuit board interconnect based on embedded graded-index planar glass waveguides," J. Lightw. Technol., vol. 33, no. 4, pp. 741–754, Feb. 2015.
- [16] Y. Vlasov, W. M. J. Green, and F. Xia, "High-throughput silicon nanophotonic wavelength-insensitive switch for on-chip optical networks," *Nature Photon.*, vol. 2, no. 4, pp. 242–246, Mar. 2008.
- [17] M. Lipson, "Guiding, modulating, and emitting light on silicon-challenges and opportunities," *J. Lightw. Technol.*, vol. 23, no. 12, pp. 4222–4238, Dec. 2005.
- [18] M. Immonen et al., "End-to-end optical 25 Gb/s link demonstrator with embedded waveguides, 90° out-of-plane connector and on-board optical transceivers," in Proc. 42nd Eur. Conf. Opt. Commun., Dusseldorf, Germany, 2016, pp. 1–3.
- [19] P. Maniotis et al., "Application-oriented on-board optical technologies for HPCs," J. Lightw. Technol., vol. 35, no. 15, pp. 3197–3213, Aug. 2017.
- [20] HDP User Group International, Inc. Optoelectronics project, 2010. [Online]. Available: http://hdpug.org/optoelectronics
- [21] R. Pitwon et al., "International standards for optical circuit board fabrication, assembly and measurement," Opt. Commun., vol. 362, pp. 22–32, Mar 2016
- [22] M. P. Immonen et al., "Single-mode polymer waveguide PCBs for on-board chip-to-chip interconnects," Proc. SPIE OPTO, vol. 10109, 2017, Art. no. 101090K.
- [23] D. M. Kuchta et al., "A 56.1 Gb/s NRZ modulated 850 nm VCSEL-based optical link," in *Proc. Opt. Fiber Commun. Conf.*, Anaheim, CA, USA, 2013, pp. 1–3.
- [24] P. Westbergh, E. P. Haglund, E. Haglund, R. Safaisini, J. S. Gustavsso, and A. Larsson, "High-speed 850 nm VCSELs operating error free up to 57 Gbit/s," *Electron. Lett.*, vol. 49, no. 16, pp. 1021–1023, Aug. 2013.

- [25] X. Xu, L. Ma, W. Zhang, J. Du, and Z. He, "Fabrication and performance analysis of polymer waveguides for optical interconnects," in *Proc. IEEE Opt. Interconnects*, 2016, pp. 76–77.
- [26] D. H. Sim, Y. Takushima, and Y. C. Chung, "High-speed multimode fiber transmission by using mode-field matched center-launching technique," *J. Lightw. Technol.*, vol. 27, no. 8, pp. 1018–1026, Apr. 2009.
- [27] N. Bamiedakis, J. Chen, R. V. Penty, and I. H. White, "Bandwidth studies on multimode polymer waveguides for ≥25 Gb/s optical interconnects," *IEEE Photon. Technol. Lett.*, vol. 26, no. 20, pp. 2004–2007, Oct. 2014.
- [28] N. Bamiedakis et al., "40 Gb/s data transmission over a 1-m-long multi-mode polymer spiral waveguide for board-level optical interconnects," J. Lightw. Technol. vol. 33, no. 4, pp. 882–888, Feb. 2015.
- [29] J. Chen, N. Bamiedakis, P. Vasil'ev, R. V. Penty, and I. H. White, "Bandwidth enhancement in multimode polymer waveguides using waveguide layout for optical printed circuit boards," in *Proc. Opt. Fiber Commun. Conf.*, Anaheim, CA, USA, 2016, paper W1E.3.
- [30] N. Bamiedakis et al., "56 Gb/s PAM-4 data transmission over a 1 m long multimode polymer Interconnect," in Proc. Conf. Lasers Electro-Opt., San Jose, CA, USA, 2015, paper STu4F.5.
- [31] N. Bamiedakis, J. Beals, R. V. Penty, I. H. White, J. V. DeGroot, and T. V. Clapp, "Cost-effective multimode polymer waveguides for high-speed on-board optical interconnects," *IEEE J. Quantum Electron.*, vol. 45, no. 4, pp. 415–424, Apr. 2009.

Xiao Xu was born in Shandong, China, in 1992. She received the B.S. degree in electronic science and technology from the University of Electronic Science and Technology of China, Chengdu, China, in 2014. She is currently working toward the Ph.D. degree at Shanghai Jiao Tong University, Shanghai, China. Her major research interests include optical interconnects and optical waveguide devices.

Lin Ma (M'09) received the B.S. degree from Wuhan University of Technology, Wuhan, China, in 2003, and the M.S. and Ph.D. degrees in electrical communication engineering from Tohoku University, Sendai, Japan, in 2006 and 2009, respectively. In 2010, he joined the NTT Access Network Service Systems Laboratories, NTT Corporation, Tsukuba, Japan, where he was engaged in research on specialty optical fibers. Since 2014, he has been an Associate Professor with Shanghai Jiao Tong University, Shanghai, China. His research interests include specialty optical fibers and waveguides for optical transmission and sensing applications.

Marika Immonen (M'05) received the M.S. degree from Helsinki University of Technology (HUT) in 2003 in the field of Electronics Production and Reliability Engineering, and became Researcher in HUT for 2002–2005 studying optical waveguide materials, board-level interconnects, and photonics reliability. Thereafter she joined Aspocomp Group to develop production processes for photonic PCB. In 2008, she joined TTM Technologies to lead engineering team developing advanced PCB products with embedded optical interconnects. She is well-recognized expert in the field, has authored numerous conference and journal papers, and is a Member of SPIE. She has been nominated as an expert member on the National Electro-technical Standardization Organization (SESKO) Fibre Optics committee, and International Electro-technical Commission Standards subcommittees.

Xinhong Shi (M'06) received the B.S. degree from Nantong University, Nantong, China, in 2004, and the M.S. degrees in physical chemistry from Shanghai University, Shanghai, China in 2007. Since that she has been working in TTM Technologies in the Department of Advanced Development. She worked for advanced printed circuit board process for a long time. She is currently absorbed in the optical waveguides technology for different application, backplane, line card, transceivers, Si-Photonics, etc.

Brandon W. Swatowski received the B.S. degree in electrical engineering and applied physics and the M.S. degree in electrical engineering from Michigan Technological University, Houghton MI, USA, in 2009 and 2017, respectively. In 2011, he joined Dow Corning, where he engaged in research of advance polymer systems for the fabrication of waveguide devices. Since 2016, he has been an application development engineer for The Dow Chemical Company, focused on UV curable silicones for optical applications.

Jon V. DeGroot received the Ph.D. degee in chemical engineering from the University of Minnesota, the B.S. degree from Iowa State University, and joined Dow Corning in 1994. He is recognized for his expertise in elastomer reinforcement, rheology, and the optical properties of silicones. The majority of his career has been spent in applied research and driving front-end innovation activities for Dow Corning. He began working in the area of photonics in 2001 and has championed the use of silicones for optical data communications and optics for lighting. He has authored more than 30 external publications, and has been granted 14 US patents.

Zuyuan He (M'00-SM'11) received the B.S. and M.S. degrees in electronic engineering from Shanghai Jiao Tong University, Shanghai, China, in 1984 and 1987, respectively, and the Ph.D. degree in optoelectronics from the University of Tokyo, Tokyo, Japan, in 1999. He joined the Nanjing University of Science and Technology, Nanjing, China, as a Research Associate, in 1987, and became a Lecturer in 1990, where he was engaged in the research of fiber optic sensors, evaluation and measurement of optical devices, and optical instrumentation. From 1995 to 1996, he was a Research Fellow with the Research Center for Advanced Science and Technology, University of Tokyo, involved in the research on optical information processing. In 1999, he became a Research Associate of the University of Tokyo, on measurement and characterization of fiber optic components and systems, fiber optic reflectometry, fiber optic sensors, and multidimensional optical information processing. In 2001, he joined CIENA Corporation, Linthicum, MD, USA, as a Lead Engineer responsible for optical testing and optical process development. He was with the University of Tokyo as a Lecturer in 2003, and became an Associate Professor in 2005. He was a Professor at the Center of Excellence in Electrical and Electronic Engineering, University of Tokyo. Since 2012, he has been with Shanghai Jiao Tong University as a Distinguished Professor. His current research interests include optical fiber sensors, optical fiber measurement, and optical information processing. He is a Member of the Institute of Electronics, Information, and Communication Engineers of Japan.